EPJ Web of Conferences **140**, 02020 (2017) DOI: 10.1051/epjconf/201714002020
Powders & Grains 2017

Experimental measurement of granular fabric and its evolution under shearing

Max Wiebicke[1,2,3,⋆], *Edward* Andò[1,2], *Erminio* Salvatore[1,2,4], *Gioacchino* Viggiani[1,2], and *Ivo* Herle[3]

[1] *Univ. Grenoble Alpes, 3SR, F-38000 Grenoble, France*
[2] *CNRS, 3SR, F-38000 Grenoble, France*
[3] *Technische Universität Dresden, Institute of Geotechnical Engineering, Germany*
[4] *University of Cassino, Cassino, 03043, Italy*

Abstract. X-ray μ computed tomography (CT) made three-dimensional in-situ imaging of natural granular materials possible. Previous work using x-ray μCT and triaxial compression tests has studied the 3D kinematics of individual grains during shear banding [1]. This works aims to supplement these measurements of kinematics with the measurement of different fabric entities, such as particle or contact orientations. It was found that the individual orientations of the different fabric entities pick up on the forming and the direction of the evolving shear band. The evolution of the anisotropy of the bulk of orientations corresponds to the macroscopic behaviour during the shearing test.

1 Introduction

Extracting fabric in natural granular materials has been the subject of many studies since a long time [2]. However, due to technical limitations these studies were either only possible on perfect model materials, post-mortem specimen or in numerical simulations. With the rise of x-ray μ computed tomography (CT) these limitations have been pushed to new horizons. X-ray μCT enables the acquisition of three-dimensional images of intact specimens at certain resolutions. The accuracy of the measurement of different fabric entities, such as contact and particle orientations, is increased with increasing resolution of these images. However, a trade-off between the resolution and the size of the specimen has to be made, in order to stay mechanically representative [3]. Due to these limited resolutions, some problems e.g. in the detection of contacts and the determination of their orientation arise [4, 5]. Using standard approaches of treating such images yielded several problems such as e.g. the systematic over-detection of contacts or a strong bias of the determined contact orientations. Improvements of these approaches have been suggested [5].

In this study, the fabric is extracted from tomographic images of an experiment on a real natural granular material using improved image analysis tools and it is related to the emergence of a shear band.

2 The experiment

The experiment in this study is a triaxial compression test on a dry Hostun sand at a confining pressure of 100 kPa.

⋆e-mail: max.wiebicke@tu-dresden.de

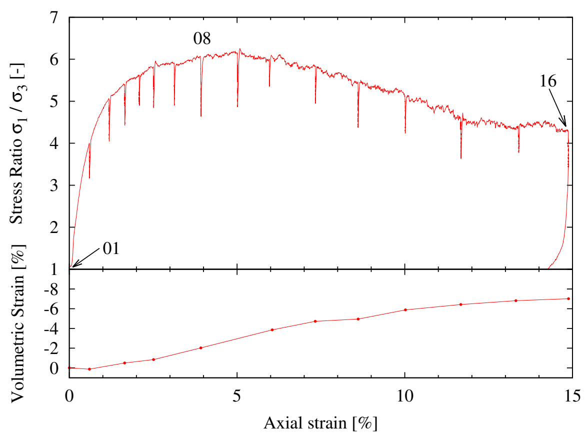

Figure 1. Macroscopic results of the triaxial compression test

The specimen was prepared by pluviation with a resulting initial relative density of 83.2%. More information on the experiment can be found in [1, 6]. In order to be able to identify individual grains in the tomographic images acquired throughout the test, the size of the specimen was chosen to be relatively small (height = 24.31 mm, diameter = 10.70 mm) with the images being acquired at a resolution of 15 μm/pixel.

The macroscopic response of the specimen is plotted in Figure 1. Images were acquired throughout the experiment with x-ray μ-CT; the relaxation parts of the stress-strain behaviour correspond to the states at which the experiment was paused and the images were acquired.

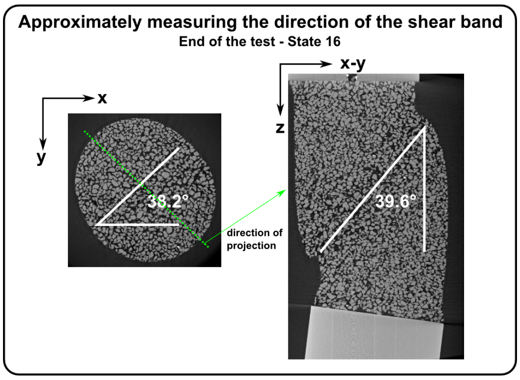

Figure 2. Measuring the orientation of the shear band in spherical coordinates

A single shear band formed during the compression test. Its orientation in the final state (16) in spherical coordinates was measured to be $\phi \approx 51.8°$ and $\theta \approx 50.4°$ with ϕ being the azimuthal angle and θ being the polar angle, see Figure 2.

3 Measuring fabric

In order to extract the two chosen fabric entities, contact and particle orientations, different approaches were chosen and will be explained in the corresponding sections. The images published in [1] have been used as input for the image processing. As described in [1], the initial grey-scale image (with the grey-values corresponding to x-ray attenuation and thus, mass density) is first binarised based on a physical threshold. The particles in this binary image are then separated using the high speed 3D Watershed algorithm mentioned in [1] and labelled. Using the labelled image, a connectivity, describing which particles are in contact with each other, can be determined; this procedure is outlined in [6].

Only two subsets of the sample are considered in the present study. One subset is located to capture a part of the evolving shear band, the other is well outside the shear band, close to the top platen of the specimen. Each subset has a size of 300x300x300 pixels, corresponding to 4.5x4.5x4.5 mm, and containing 1230 to 1743 particles at different stages of the test. To follow the evolution of fabric in both subsets throughout the test, three different states are chosen: 01 - the initial state, 08 - peak stress state, 16 - the end of the experiment.

In order to statistically express and gather the individual orientations, a second order fabric tensor [7] is used:

$$\mathbf{F} = \frac{1}{N} \sum_{i \in N} \mathbf{o}_i \otimes \mathbf{o}_i \tag{1}$$

with $\mathbf{o}_i$ being an individual orientation and N being the number of orientations. The difference between the first and third eigenvalue of the tensor $\mathbf{F}$ was chosen to be a measure for the anisotropy and a way to follow the evolution throughout the test.

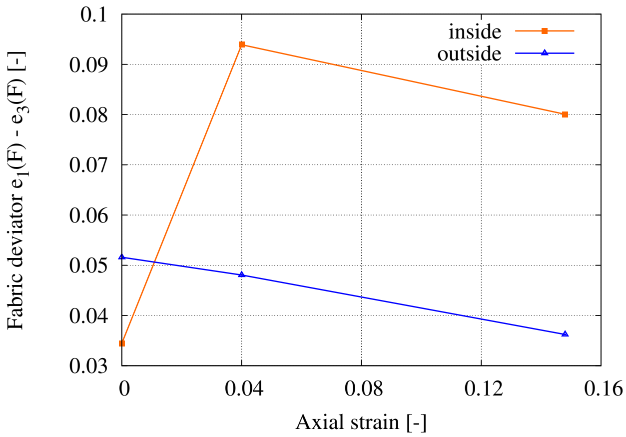

Figure 3. Evolution of the deviatoric contact fabric

3.1 Contact orientations

In order to deal with the systematic over-detection of contacts when using standard approaches as the one described above, a local refinement is applied on the contacts that were detected [5]. Within this approach, a local threshold (that is higher than the global one) is applied on every contact in the connectivity for improvement, i.e. if the corresponding particles do not appear to be in contact after applying the local threshold, the contact is deleted from the connectivity. The orientation of the contacts, which is defined as a normal to the contact plane, is then assessed using the random walker, an advanced watershed algorithm [4, 8].

The individual contact orientations of both subsets in the three chosen states are plotted in Figure 4. The contact orientations in the initial state appear to be either mostly vertical or horizontal, which corresponds to the center and the outer ring in the plots. Only some contacts are oriented in mixed directions (horizontal and vertical). That holds for the orientations in both subsets as the initial state seems to be homogeneous. In both following states, the peak (08) and the end of the test (16), the orientations correspond to the direction of the shear band. The normal to the shear band as well as the directions of the shear band are marked in Figure 4. The contact fabric outside of the shear band undergoes only minor changes with no preferable orientations.

The evolution of the deviatoric contact fabric with the macroscopic loading in the subsets is shown in Figure 3. Outside the shear band the anisotropy of the contact orientations is decreasing with increasing axial strain. In the subset inside the shear band the anisotropy is increased at the peak stress state (08) with respect to the initial state. The deviatoric contact fabric at the end of the test (16) shows a slightly lower anisotropy than at the peak stress state and it is higher than at the initial state. This evolution corresponds to the evolution of the stress ratio during shearing which is increasing until the peak state and then slightly decreasing to the end of the test, compare with Figure 1.

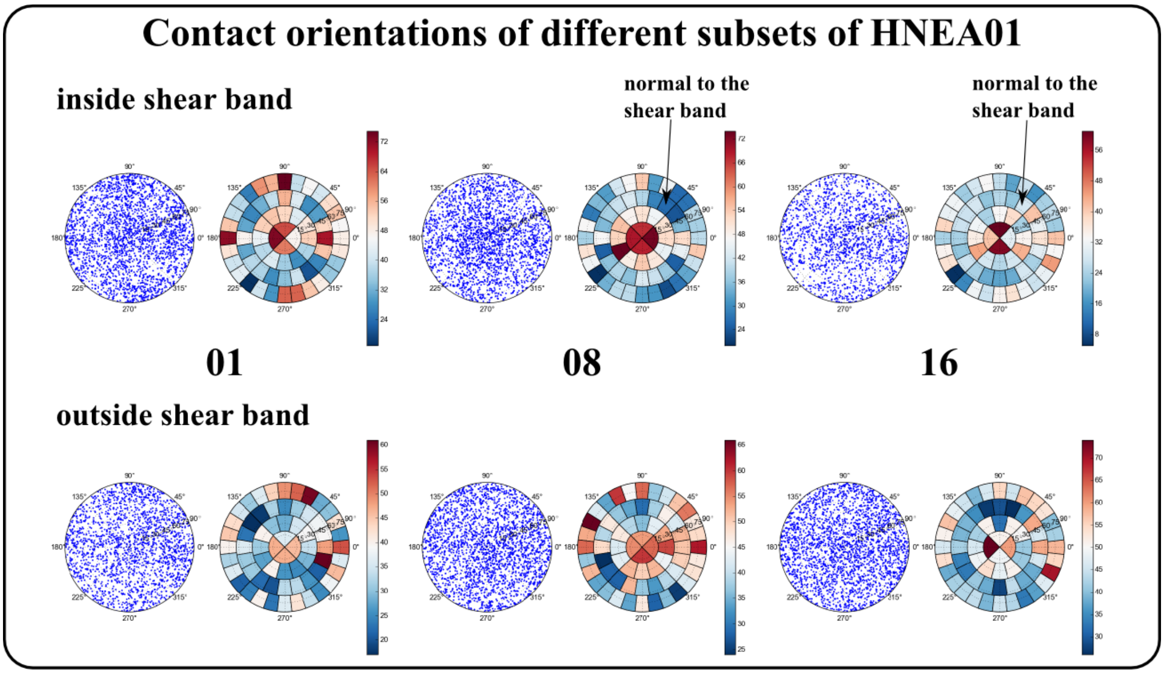

Figure 4. Plots of projected contact orientations - chosen projection: Lambert azimuthal equal area projection. Individual and binned orientations.

3.2 Particle orientations

The moment of inertia tensor was chosen for the characterisation of the particle orientations. Its eigenvectors correspond to the principal particle orientations: longest, intermediate and shortest axis. A study on the particle orientations using a high resolution scan of an individual Hostun sand grain [5] showed that in case of non-spherical particles there is usually one very clearly defined axis and two less clearly defined axes. Depending on the shape the most clearly defined axis is either the long or the short axis. In this case and in general for Hostun sand, the long axis, i.e. the eigenvector of the moment of inertia tensor corresponding to the smallest eigenvalue, is the most clearly defined axis of most particles. Thus, for consistency, this orientation is defined as the principal particle orientation for each particle.

The individual particle orientations of both subsets in the three chosen states are plotted in Figure 6. The initial states of both subsets are again very similar, with the longest axis of the particles being orientated strongly horizontal. The same still holds for the peak stress state (08) with only minor changes of the orientations. At the end of the test (16), the particles inside the shear band appear to reorientate themselves in the plane of the shear band. That however happens again at the horizontal plane with only minor vertical components of the orientations. This alignment is marked in Figure 6 as the opposite to the normal of the shear band. Outside of the shear band the particle orientations undergo only minor changes at the end of the test.

The evolution of the deviatoric particle fabric with the macroscopic loading in the subsets is shown in Figure 5.

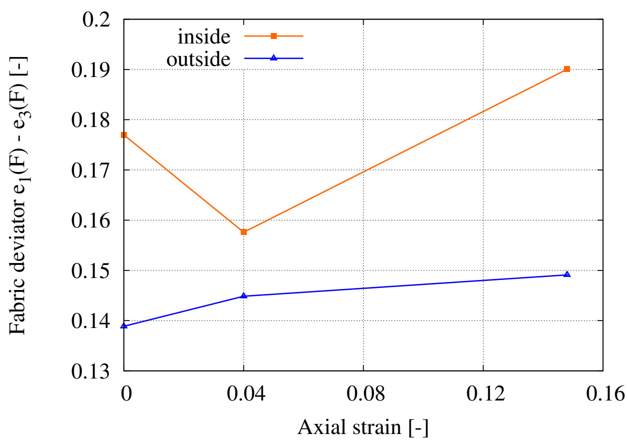

Figure 5. Evolution of the deviatoric particle fabric

The devitoric fabric outside the shear band undergoes only minor changes. Inside the shear band the anisotropy of the particle orientations at the peak stress state (08) is lower than the initial anisotropy. At the end of the test, however, the anisotropy has increased to a higher value than at the initial state. This corresponds to the observation on the individual orientations: the particle orientations do not clearly respond to the onset of the localisation at the peak state, but a tendency can be observed later at the end of the test, see Figure 6.

4 Conclusions

Different fabric entities were extracted from tomographies that were acquired throughout a triaxial compression test

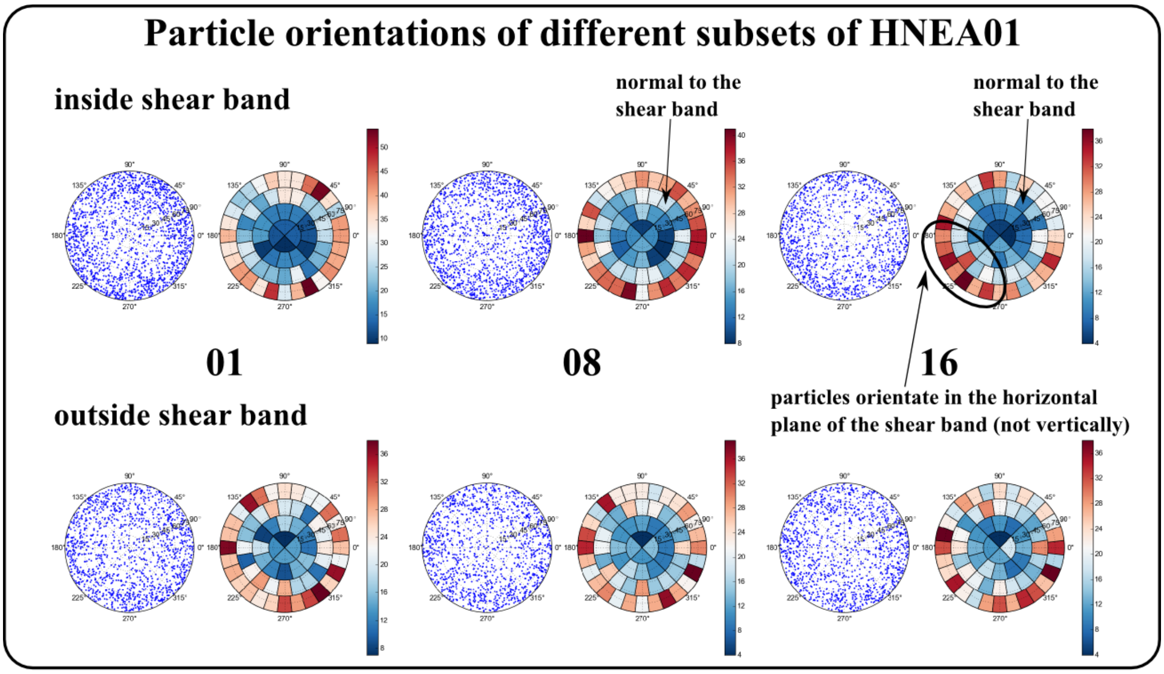

Figure 6. Plots of projected particle orientations - chosen projection: Lambert azimuthal equal area projection. Individual and binned orientations.

on Hostun sand. Using improved image analysis tools, individual contact as well as particle orientations were determined on subsets of the specimen that are located inside and outside an evolving shear band. Interparticle contacts and particle orientations align in the plane of the shear band with ongoing macroscopic shearing. Contact orientations reflected the shear band already at the peak stress state whereas particle orientations appear to pick up the shear band with a delay.

The evolution of anisotropy of the contact fabric inside the shear band corresponds to the evolution of stress, increasing up to the peak stress and decreasing slightly afterwards. The particle fabric picked up the later alignment with the shear plane but showed no clear evolution.

However, the second order approximation of the fabric tensor is limited as shown in [7] and a further study will investigate the need for higher order approximations. Another limiting factor might be the choice of the measure of anisotropy. Different invariants of the fabric tensor are subject of another study. Furthermore, the whole specimen with all its particles and contacts will be investigated by the same means.

Acknowledgements

Laboratoire 3SR is part of the LabEx Tec 21 (Investissements d'Avenir - grant agreement n°ANR-11-LABX-0030). The research leading to these results has received funding from the European Research Council under the European Union's Seventh Framework Program FP7-ERC-IDEAS Advanced Grant Agreement n° 290963 (SOMEF) and from the German Research Foundation (DFG) n° HE2933/8-1.

References

[1] E. Andò, S.A. Hall, G. Viggiani, J. Desrues, P. Bésuelle, Acta Geotechnica (2012)

[2] M. Oda, Soils and foundations **12**, 1 (1972)

[3] E. Andò, G. Viggiani, S.a. Hall, J. Desrues, Géotechnique Letters **3**, 142 (2013)

[4] C. Jaquet, E. Andó, G. Viggiani, H. Talbot, *Estimation of Separating Planes between Touching 3D Objects Using Power Watershed*, in *International Symposium on Mathematical Morphology* (2013), Vol. 11, pp. 452–463

[5] M. Wiebicke, E. Andó, G. Viggiani, I. Herle, *Towards the measurement of fabric in granular materials with x-ray tomography*, in *Proceedings of the 6th international Symposium on Deformation Characteristics* (2015)

[6] E. Andò, Ph.D. thesis, Université de Grenoble (2013)

[7] K.I. Kanatani, International Journal of Engineering Science **22**, 149 (1984)

[8] L. Grady, *Random walks for image segmentation*, in *IEEE Transactions on Pattern Analysis and Machine Intelligence* (2006), Vol. 28